Asian Journal of Applied Science and Technology (AJAST)
Volume 10, Issue 1, Pages 13-36, January-March 2026

Investigating the Spatial Distribution, Environmental Pathways, and Public Health Risks of Natural Radioactivity in Khulna Division, Bangladesh

Upendra Sen Chakma[1*], Joy Chandro Roy[2], Chandrika Mondol[3], Ayon Chakrobortty[4] & Md. Abadat Hossain[5]

[1,3,4]*Physics Discipline, Khulna University, Khulna 9208, Bangladesh.* [2]*Department of Physics, Khulna University of Engineering and Technology, Khulna 9203, Bangladesh.* [5]*Department of Natural Science, Port City International University, Chittagong, Bangladesh.*
Corresponding Author (Upendra Sen Chakma) Email: upendrasenchakma@gmail.com[*]

DOI: https://doi.org/10.38177/ajast/2026.10102

Article Received: 09 November 2025 *Article Accepted: 14 January 2026* *Article Published: 22 January 2026*

ABSTRACT

In this review, we attempt to investigate the environmental pathways, public health risks, and spatial distribution of naturally occurring radioactivity across the Khulna Division, Bangladesh. With previous measurements of radionuclides like ^{226}Ra, ^{232}Th and ^{40}K from various environmental sources like soil, sediment, dust, papaya, rice, leafy vegetables and arum, the study represents the first regional radiological contamination assessment. We have used data from previous studies in this review and Geographic Information System (GIS) mapping was utilized to explore spatial variations and radiological hotspots across the region. Sediment samples from Bagerhat and Satkhira show the highest activity concentrations, with ^{226}Ra reaching 101.3 Bqkg^{-1}, ^{232}Th at 115.3 Bqkg^{-1}, whereas ^{40}K exceeding 16,000 Bqkg^{-1}. Radiological hazard indices Ra_{eq} reaches at 1518 Bqkg^{-1} and Excess Lifetime Cancer Risk (ELCR) exceeds 3×10^{-3} surpassed the global safety standard limits showing significant risks for public health living across the region and populations may get exposed for extended periods whereas food samples indicating the low radioactivity transfer from soil to plant. These results highlight the necessity for further monitoring in those places with high radioactivity levels associated with shifting agricultural and environmental conditions. The study serves as a reference for future radioactivity survey in a broader scale for environmental sustainability, radiation safety, and public health care in the ecologically fragile region of Bangladesh.

Keywords: Radioactivity; Radionuclides; Activity Concentrations; Gamma Spectrometry; Radiological Health Assessment; Pathways in the Environment; Geographic Information System; Excess Lifetime Cancer Risk; Annual Average Committed Effective Dose.

1. Introduction

Radioactivity is a fundamental, although inconspicuous part of our environment that results from natural and anthropogenic processes. Naturally occurring radionuclides such as Uranium (^{238}U), Thorium (^{232}Th), Radium (^{226}Ra) and Potassium (^{40}K) have been present since the Earth was formed, provide a steady background radiation in soil, rocks, water, air, dust, sediments and food products (Mitrović et al., 2016; Shahbazi-Gahrouei et al., 2013). These naturally occurring radioactive materials (NORMs) are taken up by the ecosystem and food chains of humans through various environmental matrixes including soil, water, sediment, atmospheric dust fall, and plant products such as papaya (*Carica papaya*), paddy rice (*Oryza sativa*), leafy vegetables, and arum (Absar et al., 2014; Rashed-Nizam et al., 2014). In the natural environment, the presence and mobility of radionuclides is of special pervasiveness for long-term exposure due to its high concentration. It may cause significant radiological health risks such as cancer, genetic mutations, and organ dysfunction (Yang et al., 2025). Additionally, human activities, including industrial processes, agriculture (phosphate fertilizers), coal power plants and medical applications of ionizing radiation, introduce anthropogenic nuclides, increasing the flux threatening the environment and public health trends (Mitrović et al., 2016; Mphaga & Rathebe, 2026; Yang et al., 2025). Therefore, investigating spatial distribution patterns of environmental pathways of radionuclides and the relationship between radionuclide exposure and high-risk groups (specific age group) is important for management of the natural environment under threat and to consider health care policy, especially in ecologically exposed areas like Khulna Division (Choudhury et al., 2022; Siraz et al., 2025). Bangladesh is located inside the Bengal Basin, a place formed via sedimentological procedures driven by way of the Ganges-Brahmaputra-Meghna (GBM) river system, which impacts the distribution

of heavy minerals and naturally occurring radionuclides in the environment (Siraz et al., 2025). Khulna division, the southwestern part of Bangladesh, is characterized by its deltaic panorama encompassing numerous ecosystems consisting of the Sundarbans mangrove forest, fertile agricultural lands, complex rivers and tidal structures, in addition to business and urban facilities. The region's Quaternary sediments are recognized to include accelerated concentrations of primordial radionuclides generating herbal history gamma radiation (Absar et al., 2014; Shahbazi-Gahrouei et al., 2013). Additionally, anthropogenic sources, together with shipbreaking yards, fertilizer vegetation, and clinical facilities, make a contribution to environmental radioactivity (Siraz et al., 2025). The multifaceted pathways through which radionuclides enter the ecosystem from soil and water to airborne dust and food crops spotlight the desire to integrate environmental matrices including soil, water, sediment, dust, papaya, rice, paddy, leafy vegetables, and arum for a comprehensive understanding of radioactivity dynamics in Khulna (Dickson-Agudey et al., 2026; Ekong et al., 2021; Rashed-Nizam et al., 2014).

Despite numerous localized experimental studies measuring radioactivity in numerous environmental samples from extraordinary components of Bangladesh, together with sporadic facts in Khulna, those efforts were fragmented, focusing on confined pattern kinds or geographic regions (Kabir et al., 2009). There is currently no unified, comprehensive dataset available that integrates radioactivity measurements across all applicable environmental booths for the entire Khulna division. Moreover, existing research largely lacks spatial distribution mapping that contextualizes the geographic variability of radioactivity and infrequently deals with the complex ecological pathways via which radionuclides move (Wong et al., 2025). Significantly, the relationship between environmental radioactivity stages and human health outcomes across distinctive age businesses that have various sensitivities and publicity pathways stays underexplored (Choudhury et al., 2022; Yang et al., 2025). The absence of standardized methodologies and harmonized radiological risk assessments limits the ability to form sound conclusions and manual chance mitigation correctly. The fragmented nature of prior research, methodological inconsistencies, and limited awareness on ecosystem-level transfer create widespread gaps in knowledge. There is insufficient integration of statistics from soil, water, sediment, air dust, and regionally ate-up food items, ensuring an incomplete knowledge of the environmental fate and bioaccumulation of radionuclides (Rashed-Nizam et al., 2014; Siraz et al., 2025). Moreover, the dearth of GIS-based spatial distribution analyses prevents identity of radioactivity hotspots and the system of focused interventions (Siraz et al., 2025). Most importantly, no study has carefully correlated radioactivity levels with anticipated radiological health risks differentiated by age groups in the Khulna region (Siraz, Al Mahmud, et al., 2023; Yang et al., 2025).

Addressing these gaps is vital for specific risk characterization and development of sustainable environmental and public health policies. Studies in Bangladesh have shown that areas with sedimentary deposits containing monazite and zircon minerals show off higher natural background radiation (Mitrović et al., 2016; Rashed-Nizam et al., 2014). Investigations in Khulna and nearby areas studied radionuclide concentrations in soil, water, and sediments often exceeding worldwide average levels, although radiological hazard indices often remain underneath crucial thresholds (Absar et al., 2014; Kabir et al., 2009). After natural calamities like Cyclone Aila, changes in soil and sediment profiles have altered radioactivity ranges, posing long-term risks to regional ecosystems and communities. Industrial activities, shipbreaking yards, and medical radiation sources make a contribution to

localized artificial radionuclide inputs (Siraz et al., 2025). Airborne dust containing radioactive particles similarly allows environmental dispersion (Kabir et al., 2024; Khan et al., 2025; Siraz et al., 2025). Regardless of revealing these key insights, previous research efforts have commonly lacked comprehensive assessment of multiple environmental media mixed with demographic health risk analyses, in particular across Khulna Division (Siraz et al., 2025; Tasnim Nijhum et al., 2021).

1.1. Study Objectives

In this review we aim to:

1) Collect and synthesize all formerly published experimental data on radioactivity concentrations of natural and anthropogenic radionuclides measured experimentally in various environmental samples (soil, water, sediment, dust, papaya, paddy, leafy vegetables, arum, etc.) from all districts of Khulna Division.

2) Generate GIS-primarily based spatial distribution maps to visualize geographical variations and identify potential radioactivity hotspots across the entire region.

3) Analyze ecosystem pathways for radionuclide transfer across environmental matrices to explain mechanisms of infection and capacity bioaccumulation in food chains.

4) Check radiological hazard indices and perform age-suitable dose estimations to correlate environmental radioactivity exposure with potential health risks for various demographic groups.

This review would offer a comprehensive overview of radioactivity concentrations and radiation exposures as well as analyze the ecological pathways and impacts on public health and to establish a benchmark for environmental radioactivity and health risk assessment, identifying and addressing gaps in modern expertise and synthesizing fragmented data in Khulna Division, Bangladesh. These insightful results will provide guidance to policymakers, environmental scientists, and healthcare professionals in developing sustainable strategies for radiation protection, environmental safety, and human well-being safety guidelines amid continued industrialization and environmental conditions.

2. Methodology

2.1. Study Area and Background

Khulna Division is located in the southwestern part of Bangladesh, a region of the country known for its rivers, vibrant coastal life and the world's largest mangrove forest, Sundarbans. This region is called one of the vital areas in the country, where rapidly growing industrial progress and modern urbanization connect with sensitive eco-friendly environments. It has become one of the most strategically important regions in the southwest part of the country, because of its geographical surrounding including extensive riverine networks, coastal ecosystems, and the presence of the world's largest mangrove forest, Sundarbans (Arafin et al., 2020; Siraz, Jubair, et al., 2023). The meeting point of the two major rivers like the Rupsha and the Bhairab made the region one of the major spots in the movement and spread of both natural and man-induced contaminants (Islam, 2016; Nahar, 2016). Because of these contaminants, this area is a good place to study radioactivity in the environment. Previous studies have been carried out on a smaller scale. This research, on the other hand, looks at soil, sediment, vegetables, and dust from a wide

range of different areas. The nobility of this research is an effort to estimate overall radiation exposure hazards for this regional population by assessing combined radioactivity contamination levels across several environmental matrices in a systematic way. In order to ensure wide spatial coverage of Khulna Division, we selected those experimental studies for our review, which represent diverse sampling sites including urban, riverine, coastal, mangrove forest, rural, and agricultural environments as shown in Table 1. Khulna City, the third-largest one in Bangladesh and nearby the Rupsha River Bank has been selected for this study because of its industrial growth and vital role in the region's water system (Islam, 2016). Several ecological sites around the world largest mangrove forest, Sundarbans including Harbaria, Koromjol and Jongra, have been chosen to explore how coastal conditions and ecological factors are impacting this environment (Arafin et al., 2020; Siraz, Jubair, et al., 2023; Tasnim Nijhum et al., 2021). Remote rural and semi-urban areas such as Jashore Sadar, Chaugachha, Jhikargachha, and Veramara have been presented in this study to provide reliable regional information (Kabir et al., 2009). In addition, the Morolgonj (Bagerhat) and Koira (Khulna) these two upazilas, were selected for their strong reliance on vital eco-friendly services and risk of both natural and human-induced environmental stresses (Arafin et al., 2016). Moreover, the regions that have been taken into consideration for our review, like Khulna, Bagerhat, Satkhira, Jessore, and Kushtia, show an extensive variety of ecosystems including rural fields, vulnerable coastal wetlands, dense urban areas, and seaports. The Figure 1 represents these sample locations graphically. The industrial importance of Mongla Port, located in Bagerhat, the agricultural cultivations in Jessore and Kushtia districts, and the presence of the world's largest mangrove forest, Sundarbans, make this southwest zone of Bangladesh significantly vulnerable to environmental and radiological health risks (Ehsan et al., 2019; Kabir et al., 2009). Rapidly growing industrial development and modern urbanization across the region resulting in traffic increases, industrial emissions, land-use changes, and environmental damage intensify the necessity for continuous monitoring to safeguard environmental and public health. This regional combination of ecological, rural, coastal and urban locations for this study provides a strong framework for the spatial distribution of environmental radionuclides and the establishment link between human activities and natural processes in the Khulna Division and the adjacent districts.

Table 1. Geographical Locations of Collected Environmental and Agricultural Samples (Soil, Sediment, Dust, and Food Stuff) in Khulna Division.

Sample ID	Sites Name	Latitude	Longitude	References
Sat-S1	Shamnagar, Satkhira	22°20'27.83"	89°5'56.99"	(Arafin et al., 2020)
Sat-S2	Shamnagar, Satkhira	22°20'15.82"	89°6'17.07"	(Arafin et al., 2020)
Kh-D1	Khulna City Corporation, Khulna	22°49'6.77"	89°33'21.85"	(Khan et al., 2025)
Kh-Se1	Jongra, Khulna	22°20'30.12"	89°17'60.0"	(Tasnim Nijhum et al., 2021)
Kh-Se2	Jongra, Khulna	22°21'26.82"	89°18'4.32"	(Tasnim Nijhum et al., 2021)

Ba-Se1	Karomjol, Bagerhat	22°25’42.98”	89°35’29.93”	(Tasnim Nijhum et al., 2021)
Ba-Se2	Koromjol, Bagerhat	22°25’41.41”	89°35’25.68”	(Tasnim Nijhum et al., 2021)
Sat-Se1	Satkhira	22°43’18.52”	89°4’10.15”	(Tasnim Nijhum et al., 2021)
Sat-Se2	Satkhira	22°41’50.73”	89°4’10.46”	(Tasnim Nijhum et al., 2021)
Kh-S1	Rupsha, Khulna	22°48’6.91”	89°34’29.82”	(Islam, 2016)
Kh-Se3	Rupsha, Khulna	22°49’0.46”	89°36’34.65”	(Islam, 2016)
Kh-Pap1	Rupsha, Khulna	22°49’15.27”	89°36’22.29”	(Nahar, 2016)
Kh-Pad1	Rupsha, Khulna	22°48’14.88”	89°34’50.83”	(Nahar, 2016)
Kh-LV1	Rupsha, Khulna	22°47’30.45”	89°34’26.11”	(Nahar, 2016)
Kh-A1	Rupsha, Khulna	22°46’31.19”	89°33’14.43”	(Nahar, 2016)
Kh-A2	Rupsha, Khulna	22°47’46.40”	89°34’13.75”	(Jolly Sultana et al., 2018)
Ba-S1	Morolgonj, Bagerhat	22°27’2.79”	89°51’6.68”	(Arafin et al., 2016)
Kh-S2	Koira, Khulna	22°21’5.48”	89°17’8.74”	(Arafin et al., 2016)
Je-S1	Jessore	23°9’49.43”	89°9’36.72”	(Kabir et al., 2009)
Je-Se1	Jessore	23°11’25.44”	89°10’7.62”	(Kabir et al., 2009)
Ku-S1	Veramara, Kusthia	24°0’57.92”	88°59’39.78”	(Ehsan et al., 2019)
Je-S2	Jessore	23°10’30.34”	89°10’39.13”	(Hossain et al., 2024)
Je-R1	Jessore	23°9’21.59”	89°10’11.33”	(Hossain et al., 2024)
Kh-S2	Harbaria, Khulna	22°17’53.74”	89°36’51.48”	(Siraz, Jubair, et al., 2023)
Ba-S2	Koromjol, Bagerhat	22°40’20.46”	89°39’28.96”	(Siraz, Jubair, et al., 2023)
Kh-Pap2	Rupsha, Khulna	22°50’50.34”	89°33’58.04”	(Nahar, 2016)

*Sat- Satkhira, Kh-Khulna, Ba- Bagerhat, Je- Jessore, Ku-Kusthia *S- Soil, D- Dust, Se- Sediment, Pap- Papaya, Pad- Paddy, LV- Leafy Vegetable, A- Arum, R- Rice.

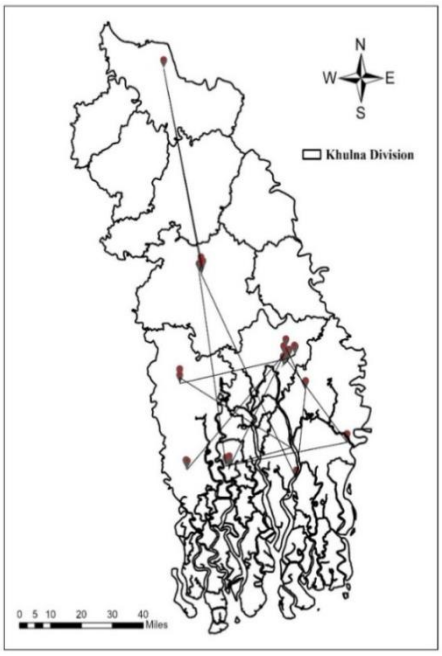

Figure 1. GIS map for sample collection locations with the help of red dots across the Khulna Division.

2.2. Sample Collection Strategy

In this paper, here all used sample value comes from various research studies that have followed strict scientific standards by particularly using High-Purity Germanium (HPGe) detectors to measure radionuclides activity concentrations. These studies were done over several decades and which ensured a reliable record of radionuclide distribution in different environments. Systematic collection of soil and sediment samples was undertaken to include both surface and subsurface layers. This was done since it was recognized that surface samples show contamination episodes that that happened recently, while subsurface layers show patterns of deposition throughout history and the radiological dynamics over long periods of time. Sample collection strategies involved spatially representative site selection across natural, agricultural, industrial, and urban areas, thereby capturing the heterogeneous contamination sources. Distances between sampling points were approximately minimal, ensuring adequate spatial resolution for trend analysis. The previous studies were conducted on food samples such as rice, leafy vegetables, and fruits like papaya. After collecting all the samples, they were sealed in a polyethylene bag or airtight container to protect them from contamination and moisture. Soil and sediment samples were weighted in kilograms to ensure a sufficient amount of sample materials for frequent and confirmatory analysis. In this review, we have used the existing radioactivity concentration data from previous experimental studies and also highlighted research gaps that haven't been addressed properly before adding new approaches that provide a more complete understanding of the radiation exposure in the region on a broader scale.

2.3. Instrumentation and Analytical Technique

All the radioactivity concentration data used in the present study were obtained by the existing studies using HPGe gamma-ray spectrometry, which is recognized as one of the global standard techniques for human-induced and naturally occurring radioactivity assessment (Chinnaesakki et al., 2012; P. J. Wallbrink, 2002). This instrument

provides exceptional energy resolution between 1.8 keV and 2.0 keV at gamma energies of 1.33 MeV. For ensuring maximum detector performance, a high-purity germanium crystal has been coupled to a cryogenic cooling system either through liquid nitrogen or an electric cooler in the HPGe system. There is an inserted preamplifier used to amplify the output signals with the help of high voltage power supply prior to the signal getting digitized through a multichannel analyzer. Finally, calibration has been done to achieve more precise and more accurate measurements in the HPGe system. Geographic Information System was integrated in this review to map and analyze naturally occurring radioactivity with the help of pinpoints of heavy radioactivity distribution patterns (Henrico et al., 2023; Kashparov et al., 2018). In this regard, first we have derived the radionuclide activity concentrations and radiological hazard indices from gamma spectrometry. Secondly, we have used those data in geolocation to their respective sampling locations and visualization using Arc GIS software. This GIS mapping approach allowed us to pinpoint the heavily radioactive contaminated hotspots. Mapping such heavily radioactive places across the region provides valuable insights into how the environmental radioactivity varies across different landscapes.

2.4. Radiological Hazard Indices

Radiological hazard indices have been estimated through calculation from the activity levels of ^{226}Ra, ^{232}Th, ^{40}K following IAEA and UNSCEAR guidelines. In this review, we calculated the Radium Equivalent Activity (Ra_{eq}), Absorbed Gamma Dose Rate (D), Annual Effective Dose Equivalent ($AEDE$) and both the External (H_{ex}) and Internal Hazard Index (H_{in}) to investigate the exposure through external and internal pathways(Eke et al., 2024; Ekong et al., 2021). In order to evaluate long-term health risks, we further estimated the Excess Lifetime Cancer Risk ($ELCR$), Annual Gonadal Dose Equivalent ($AGDE$) and age-dependent Average Annual Committed Effective Dose ($AACED$)were estimated (Lee et al., 2024; Uzochukwu Leonard & Ikenna Emmanuel, 2022). All these radiological factors are significant to address the impact of natural radionuclides and their presence made this review a vital dataset for public safety in the Khulna division, Bangladesh.

3. Result and Discussion

The activity concentrations of radionuclides ^{226}Ra, ^{232}Th, and ^{40}K from existing studies in different environmental samples from the Khulna Division in Table 2 outlines. These samples consist of soils (both surface and deep), sediments (core and bottom), dust, and food crops including papaya, paddy, rice, leafy greens, and arum. The activity concentrations of ^{226}Ra in arum range from 5.77 Bqkg^{-1} to 101.3 Bqkg^{-1} in core sediment collected from Bagerhat, while ^{232}Th levels are found to fluctuate between 2.048 Bqkg^{-1} in paddy and 115.3 Bqkg^{-1} in core sediment.

Table 2. Radioactivity concentrations of ^{226}Ra, ^{238}Th and ^{40}K radionuclides in different samples across Khulna Division

Sample Name	Sample ID	Ra-226 (Bqkg^{-1})	Th-232 (Bqkg^{-1})	K-40 (Bqkg^{-1})	References
Soil	Kh-S1	50.16±7.2	77.23±7.43	864.63±101.69	(Islam, 2016)
Soil (deep)	Sat-S1	40.65±3.92	50.61±2.78	476.62±24.51	(Arafin et al., 2020)

Soil (surface)	Sat-S2	35.59±3.94	37.69±3.92	398.73±24.19	(Arafin et al., 2020)
Soil	Ku-S1	6.3±1.33	6.63±1.29	225.4±13.31	(Ehsan et al., 2019)
Soil (surface)	Je-S1	48 ±9	53± 9	481± 78	(Kabir et al., 2009)
Soil (surface)	Kh-S2	26±3	33±6	494±25	(Siraz, Jubair, et al., 2023)
Soil (surface)	Ba-S2	27±3	39±5	540±64	(Siraz, Jubair, et al., 2023)
Soil	Je-S2	36.2 ± 0.158	42.8 ± 0.158	364.75 ± 0.791	(Hossain et al., 2024)
Soil	Ba-S1	29.275±1.69	44.34 ± 1.791	382.925 ± 20.712	(Arafin et al., 2016)
Soil	Kh-S2	41.87 ± 3.480	76.32 ± 2.653	499.905 ± 33.754	(Arafin et al., 2016)
Sediment	Kh-Se3	50.46±6.2	73.99±7.56	881.49±100.25	(Islam, 2016)
Core Sediment	Kh-Se1	54.4±11	97.8±7.5	2549.8±193.3	(Tasnim Nijhum et al., 2021)
Core Sediment	Kh-Se2	28.2±10.8	105.2±7.6	2584.6±192.7	(Tasnim Nijhum et al., 2021)
Core Sediment	Ba-Se1	101.3±13.1	115.3±9.1	16265.3±234.7	(Tasnim Nijhum et al., 2021)
Core Sediment	Ba-Se2	92.1±10.5	94.8±7.2	13291.8±190.9	(Tasnim Nijhum et al., 2021)
Core Sediment	Sat-Se1	75.4±8.2	94.3±5.8	11093.4±156.5	(Tasnim Nijhum et al., 2021)
Core Sediment	Sat-Se2	85.7±9.2	77.1±6.3	11854.7±175.8	(Tasnim Nijhum et al., 2021)
Bottom Sediment	Je-Se2	43±11	48 ± 14	503 ± 143	(Kabir et al., 2009)
Dust	Kh-D1	46.82±24.06	74.79±24.96	541.14 ± 160.79	(Khan et al., 2025)
Papaya	Kh-Pap2	43.31±15.28	15.44±11.28	1490.27±226.27	(Nahar, 2016)
Papaya	Kh-Pap1	43.31±15.28	15.44±11.28	1490.27±226.27	(Nahar, 2016)
Paddy	Kh-Pad1	24.43±5.16	2.048±2.798	93.96±133.75	(Nahar, 2016)
Rice	Je-R1	15.55 ± 0.158	19.4 ± 0.1	69.7 ± 0.570	(Hossain et al., 2024)
Leafy Vegetables	Kh-LV1	34.22±12.55	9.84±10.63	1110.50±200.24	(Nahar, 2016)
Arum	Kh-A1	5.77 ± 2.97	NA	758.298±109.66	(Nahar, 2016)
Arum	Kh-A2	5.77 ± 2.97	NA	758.298 ± 109.66	(Jolly Sultana et al., 2018)

From Table 2, it is seen that the radioactivity concentrations of ^{226}Ra varies significantly among environmental and food samples. In particular, sediment samples (Se-4 to Se-7) exhibit concentrations up to approximately 70 $Bqkg^{-1}$, with the highest value reaching 101.3 $Bqkg^{-1}$ as shown in Figure 2(a).

Table 3. The total average annual committed effective dose and Excess lifetime cancer risk for whole population for samples.

Sample ID	Whole population					
	Adult		Children		Infant	
	AACED ($mSv.y^{-1}$)	ELCR	AACED ($mSv.y^{-1}$)	ELCR	AACED ($mSv.y^{-1}$)	ELCR
Kh-Pap1	0.9 ± 0.9	3.47 ± 3.47	0.56 ± 0.57	0.31 ± 0.31	0.24 ± 0.24	0.03 ± 0.03
Kh-Pap2	0.9 ± 0.9	3.47 ± 3.47	0.44 ± 0.43	0.24 ± 0.24	0.14 ± 0.14	0.02 ± 0.02
Kh-Pad1	0.9 ± 0.9	3.47 ± 3.47	0.57 ± 0.55	0.31 ± 0.30	0.24 ± 0.23	0.03 ± 0.03
Kh-Lv1	0.9 ± 0.9	3.47 ± 3.47	0.47 ± 0.58	0.26 ± 0.32	0.17 ± 0.26	0.02 ± 0.03
Kh-A1	0.87 ± 0.9	3.34 ± 3.47	0.47 ± 0.58	0.26 ± 0.32	0.17 ± 0.26	0.02 ± 0.03
Kh-A2	0.9 ± 0.9	3.47 ± 3.47	0.48 ± 0.69	0.26 ± 0.38	0.17 ± 0.43	0.02 ± 0.05
Kh-R1	0.9 ± 0.9	3.47 ± 3.47	0.66 ± 0.44	0.37 ± 0.24	0.38 ± 0.14	0.04 ± 0.02

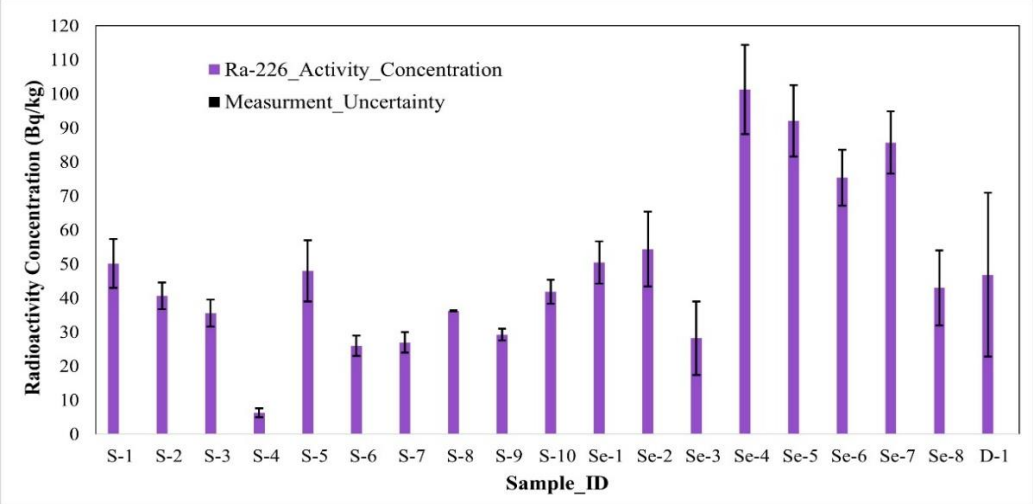

Figure 2(a). Activity concentrations of ^{226}Ra in environmental sample. Black line denotes the concentration error.

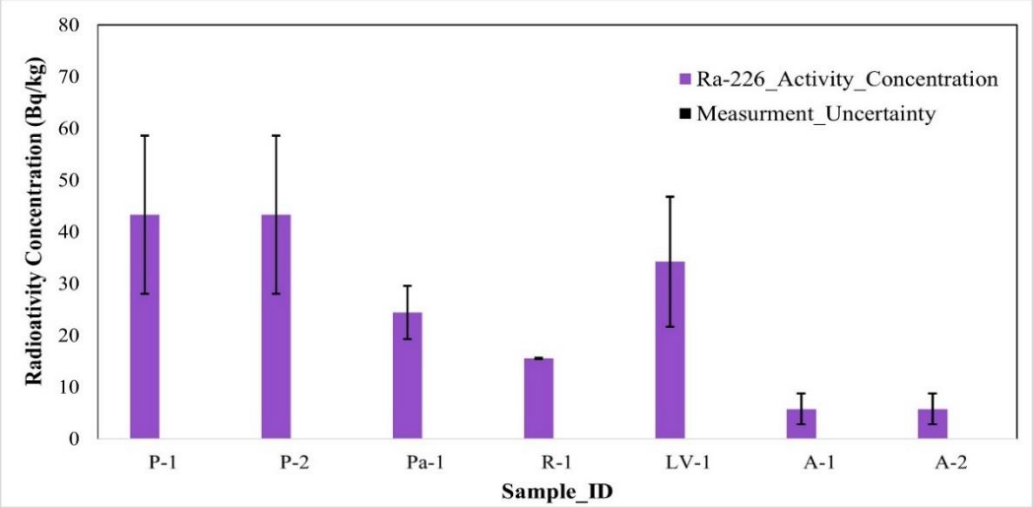

Figure 2(b). Activity concentrations of ^{226}Ra analyzed in different food samples, measured in Bq kg^{-1}.

For soil samples, the activity level is moderate from leaf vegetables, followed by arum as the lowest levels, which can be identified from Figure 2(b). This behavior can be explained by the geochemical tendency of ^{226}Ra to

accumulate in finer soil particles, along with the reliance of plants on their physiological traits and the dynamics of soil-to-plant transfer. The bar diagrams below show the difference observed in the measured activity concentrations.

The relatively low food concentrations relative to sediments indicate that there was an incomplete but yet significant transfer of the analytes from the environmental matrix due to attenuation processes which limited their uptake and hence exposure risks for human beings. Such observations suggest the necessity of continued monitoring, wider sampling and more sensitive analytic techniques to underlie radiological risk management of public health protection. In all environmental samples, which are shown in Figure 3(a), the activity concentration of ^{232}Th spans quite widely between sample types. A moderate level of radioactivity was in general recorded in soil samples (S-1 to S-10), i.e., between the ranges of 33 and 78 Bqkg^{-1}. Activity of ^{232}Th in sediment samples (Se-1 to Se-8) was significantly higher, and the highest levels were in Se-4 to Se-6 with concentration values ranging from about 94.3–115 Bqkg^{-1}. The ^{232}Th was also high in dust sample (D-1) but not as much as the most contaminated sediments.

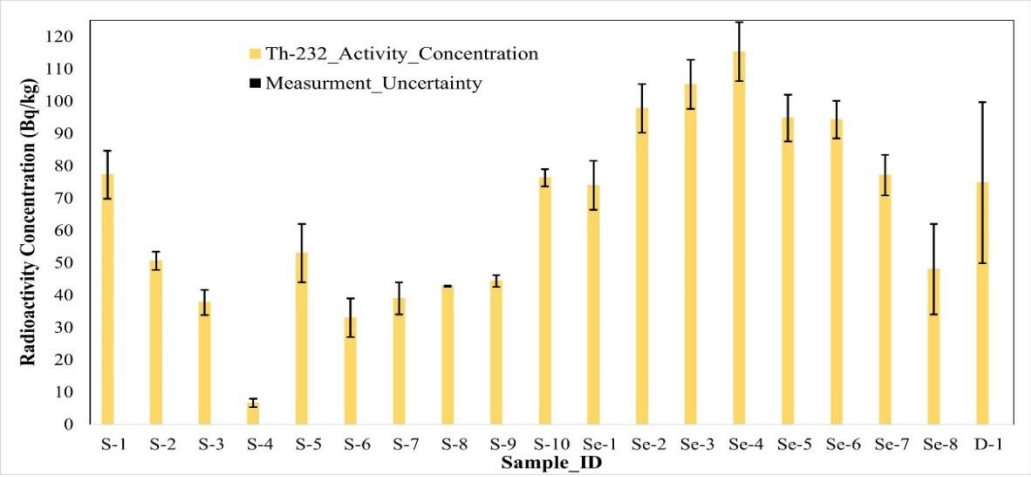

Figure 3(a). Activity concentrations of ^{232}Th in environmental samples like soil(S), sediment (Se) and dust (D), expressed in Bq kg^{-1}.

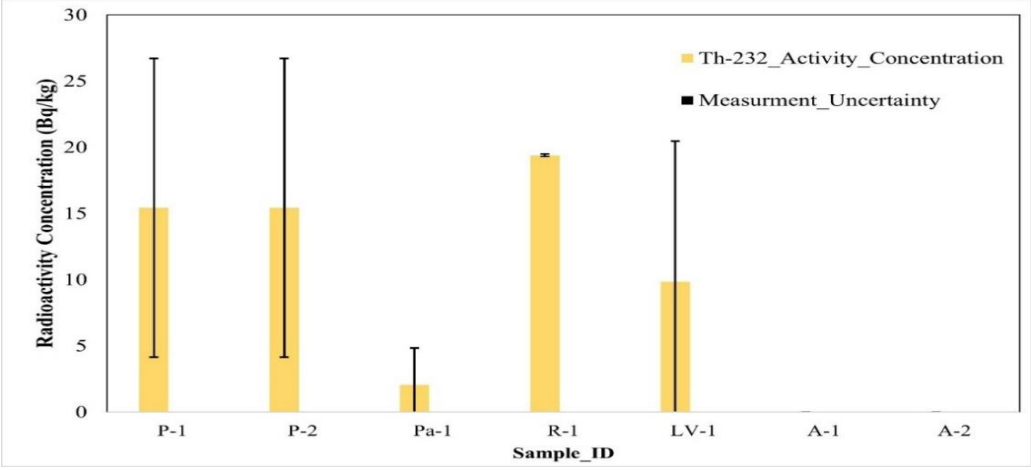

Figure 3(b). Activity concentrations of ^{232}Th measured in specific food samples, expressed in Bq kg^{-1}, showing the radioactive distribution across different samples.

On the other hand, Figure 3(b) shows ^{232}Th activity in food materials and immeasurable to low values for arum (A1-A2), while moderate values can be seen for papaya (P-1, P-2), leafy vegetables (LV-1) and paddy field rice (Pa-l) with a marked high value for Rice(R-1) whose concentrations fall within about 3 to19 Bqkg^{-1}.

This distribution highlights the preferential concentration of ^{232}Th in abiotic matrices by geochemical and deposition mechanisms that promote precipitation and adsorption. In food samples, amount of thorium (^{232}Th) is very small because plants cannot absorb it due to its weak diffusion and bioavailability, even if the environment includes high amounts (Fu et al., 2022). Absorption of differences between the species may have produced the arum samples' exceptionally low ^{232}Th values. This type of unbalanced concentrations indicates regional variability and local pollution. In general, the results indicate ^{232}Th environmental longevity and partial plant transfer, stressing that long-term monitoring and risk evaluation are essential for environmental and food safety. In Figure 4(a), moderate activity concentrations of ^{40}K measured from environmental samples which varied in the range of 225.40 - 881.49 Bqkg^{-1} (soil), which is typical natural background radiation, were obtained. The activity concentration of sediments (Se-4 and Se-7) was, however, much higher, ranging between 11,854.70 and 16,265.30 Bqkg^{-1} which may indicate concentration of the radionuclide in a distinct spot or contamination from other sources around the study area. Figure 4(b) shows the content of native radioisotope ^{40}K in food samples, and here the differences between radiometric results were remarkable according to sample type. The highest activity was in papaya and leafy vegetables, with values of 1490.27 and 1110.50Bqkg^{-1}correspondingly, these are due to their high potassium content. On the other hand, paddy and rice held the lowest levels at 93.96 and 69.7 Bqkg^{-1}, respectively.

The concentrations in the dust sample in Figure 4(a) were intermediate (541.14 Bqkg^{-1}), probably reflecting mixed soil and sediment origins. These findings confirm that ^{40}K in the environment is an actual radioactivity source to food of which soil-plant transfer pathways make available and express a potential risk of exposure through food chains. The relatively high levels of radioactivity in the sediments need to be investigated for their source and potential environmental and health risk.

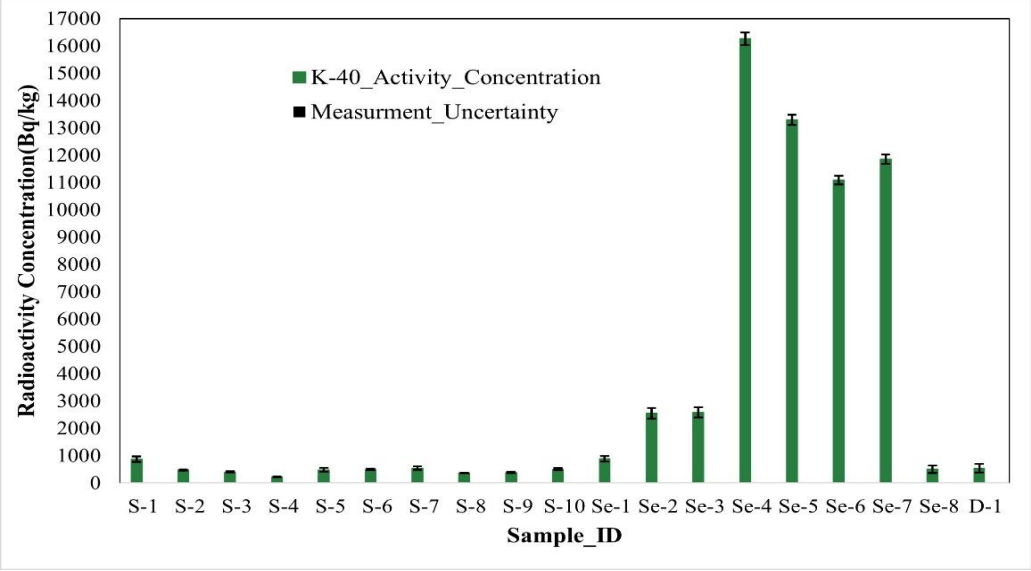

Figure 4(a). Activity concentrations of ^{40}K in environmental samples. Here comparative radioactive concentration of K is higher in sediment (Se) rather than soil (S) and dust (D).

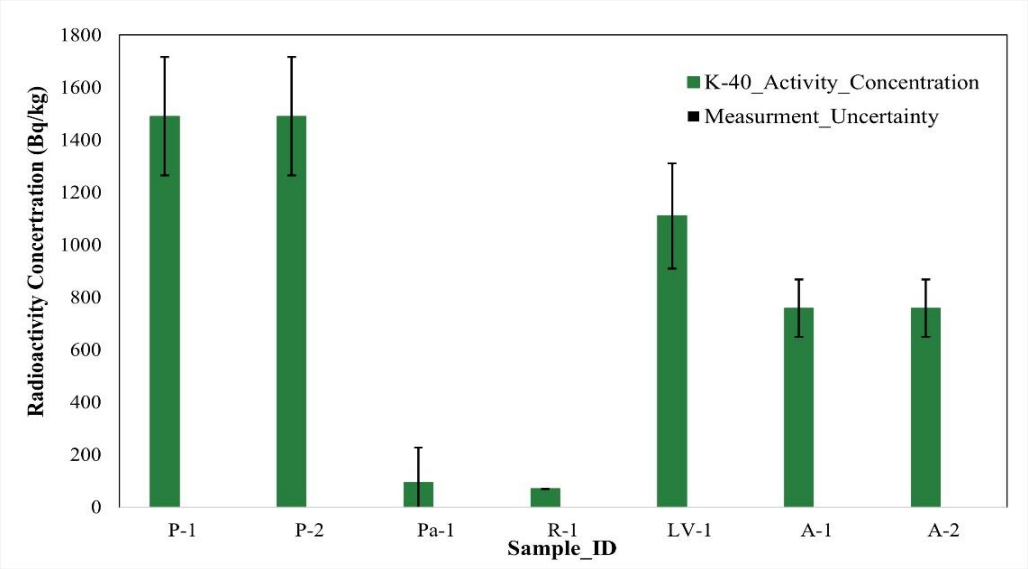

Figure 4(b). Activity concentrations of ^{40}K in different food samples with uncertainties, expressed the radioactivity in Bq kg^{-1}.

This kind of spatial variation should remind us to have a comprehensive monitoring prospect of natural radionuclide distribution as well as food safety in this region. In summary, we can say that the findings and results from Table 2 and the bar diagrams above reflect different types of hotspot contamination, which give us quite opposite in terms of transfer efficiencies and emphasize once more how important constant control is in the context of public health and food safety across the Khulna region. The internal and external radiological hazard indices as well as radiation parameters for environmental and food samples are shown in Table 4 which have been derived from the existing data on Khulna Division, Bangladesh. The absorbed gamma dose rate, annual effective dose, radium equivalent activity, external hazard index and internal hazard index were summarized and the gamma index, alpha index and excess lifetime cancer risk with value of annual gonadal dose equivalent are all given in Table 4.

Results show the higher levels of radio activity are obtained in sediment samples particularly from Bagerhat (Ba-Se1 and Ba-Se2) with computed Ra_{eq} values 1518.61 $Bqkg^{-1}$ and 1251.13 $Bqkg^{-1}$, D_{out} 794.7 $nGyh^{-1}$ at ELCR higher than 3×10^{-3} which are three orders of magnitude times greater than international recommendation criteria according to (UNSCEAR, 2000). On the other hand, arum, paddy, and rice are affected less radiologically due to the cut-off criterion of Ra_{eq} at 65 $Bqkg^{-1}$ and that of ELCR higher than 1×10^{-4} value making their values within acceptable limit. The increased sediment indices are indicative of those areas with high radionuclides concentration because of the deltaic sediment aggradation and contributions from industrial or riverine discharges, as reported previously (Arafin et al., 2020; Tasnim Nijhum et al., 2021). The values of AGDE being higher than 5000 μSvy^{-1} (Ba-Se1) revealed possible risks in reproduction and genetics in those who reside for extended periods. On the other hand, relatively low food-chain transfer factors indicated that biological uptake was limited for radionuclides, though continuous monitoring was necessary to ensure long-term food safety.

Collectively, these findings highlight a spatial heterogeneity and the urgency for targeting interventions to high-risk areas in Khulna Division. Based on these crucial salinity data, a more in-depth analysis displays important trends regarding geographical distribution, ecosystem interactions and relevance for human health assessment.

Table 4. Internal And External Radiological Hazard Indices for different samples.

Sample ID	D_{out} (nGy/h)	D_{eff} (mSv/ year)	H_{ext}	H_{in}	R_{aeq} (Bq/Kg)	Gamma Index	Iα	ELCR	AGDE
Sat-S1	69.22 ± 4.51	0.08 ± 0.01	0.4 ± 0.03	0.51 ± 0.04	149.72 ± 9.78	0.55 ± 0.04	0.2 ± 0.02	0.3 ± 0.02	486.82 ± 31.43
Sat-S2	55.83 ± 5.2	0.07 ± 0.01	0.32 ± 0.03	0.42 ± 0.04	120.19 ± 11.41	0.44 ± 0.04	0.18 ± 0.02	0.24 ± 0.02	392.72 ± 36.16
Kh-D1	89.37 ± 32.9	0.11 ± 0.04	0.53 ± 0.19	0.65 ± 0.26	195.44 ± 72.13	0.71 ± 0.26	0.23 ± 0.12	0.38 ± 0.14	627.21 ± 229.17
Kh-Se1	190.53 ± 17.67	0.23 ± 0.02	1.05 ± 0.10	1.2 ± 0.13	390.59 ± 36.61	1.52 ± 0.14	0.27 ± 0.06	0.82 ± 0.08	1377.54 ± 126.04
Kh-Se2	184.35 ± 17.62	0.23 ± 0.02	1.02 ± 0.10	1.1 ± 0.13	377.65 ± 36.51	1.48 ± 0.14	0.14 ± 0.05	0.79 ± 0.08	1338.44 ± 125.65
Ba-Se1	794.7 ± 21.34	0.97 ± 0.03	4.1 ± 0.12	4.37 ± 0.15	1518.61 ± 44.18	6.34 ± 0.17	0.51 ± 0.07	3.41 ± 0.09	5902.28 ± 152.21
Ba-Se2	654.08 ± 17.16	0.8 ± 0.02	3.38 ± 0.10	3.63 ± 0.12	1251.13 ± 35.5	5.21 ± 0.13	0.46 ± 0.05	2.81 ± 0.07	4854.48 ± 122.48
Sat-Se1	554.37 ± 13.82	0.68 ± 0.02	2.87 ± 0.08	3.08 ± 0.10	1064.41 ± 28.54	4.42 ± 0.11	0.38 ± 0.04	2.38 ± 0.06	4110.36 ± 98.72
Sat-Se2	580.47 ± 15.39	0.71 ± 0.02	2.99 ± 0.09	3.23 ± 0.11	1108.71 ± 31.75	4.62 ± 0.12	0.43 ± 0.05	2.49 ± 0.07	4309.25 ± 109.96
Kh-S1	105.88 ± 12.05	0.13 ± 0.01	0.61 ± 0.07	0.75 ± 0.09	227.18 ± 25.66	0.84 ± 0.10	0.25 ± 0.04	0.45 ± 0.05	749.31 ± 85.24
Kh-Se3	104.76 ± 11.61	0.13 ± 0.01	0.61 ± 0.07	0.74 ± 0.08	224.14 ± 24.73	0.83 ± 0.09	0.25 ± 0.03	0.45 ± 0.05	741.99 ± 82.24
Kh-Pap1	91.48 ± 23.31	0.11 ± 0.03	0.49 ± 0.13	0.6 ± 0.17	180.14 ± 48.83	0.72 ± 0.18	0.22 ± 0.08	0.39 ± 0.1	666.31 ± 165.41
Kh-Pad1	16.44 ± 9.65	0.02 ± 0.01	0.09 ± 0.05	0.16 ± 0.07	34.59 ± 19.46	0.12 ± 0.08	0.12 ± 0.03	0.07 ± 0.04	113.55 ± 69.64
Kh-LV1	68.06 ± 16.40	0.08 ± 0.02	0.36 ± 0.1	0.45 ± 0.13	133.8 ± 35.47	0.53 ± 0.13	0.17 ± 0.06	0.29 ± 0.07	495.57 ± 114.69
Kh-A1	34.29 ± 5.94	0.04 ± 0.01	0.17 ± 0.03	0.19 ± 0.04	64.16 ± 11.41	0.27 ± 0.05	0.03 ± 0.01	0.15 ± 0.03	255.93 ± 43.61
Kh-A2	34.29 ± 5.94	0.04 ± 0.01	0.17 ± 0.03	0.19 ± 0.04	64.16 ± 11.41	0.27 ± 0.05	0.03 ± 0.01	0.15 ± 0.03	255.93 ± 43.61
Ba-S1	56.27 ± 2.73	0.07 ± 0.00	0.33 ± 0.02	0.41 ± 0.02	122.17 ± 5.85	0.45 ± 0.02	0.15 ± 0.01	0.24 ± 0.01	396.04 ± 19.24
Kh-S2	52.54 ± 6.05	0.06 ± 0.01	0.3 ± 0.04	0.37 ± 0.04	111.23 ± 13.51	0.42 ± 0.05	0.13 ± 0.02	0.23 ± 0.03	373.4 ± 42.20
Je-S1	74.25 ± 12.85	0.09 ± 0.02	0.43 ± 0.08	0.56 ± 0.10	160.83 ± 27.88	0.59 ± 0.10	0.24 ± 0.05	0.32 ± 0.06	520.89 ± 89.92
Je-Se1	69.83 ± 19.50	0.09 ± 0.02	0.41 ± 0.11	0.52 ± 0.10	150.37 ± 42.03	0.55 ± 0.15	0.22 ± 0.00	0.3 ± 0.08	491.45 ± 137.41
Ku-S1	16.31 ± 1.95	0.02 ± 0.00	0.09 ± 0.01	0.11 ± 0.01	33.14 ± 4.20	0.13 ± 0.02	0.03 ± 0.00	0.07 ± 0.01	117.96 ± 13.68

Je-S2	57.79 ± 0.20	0.07 ± 0.00	0.34 ± 0.00	0.44 ± 0.00	125.49 ± 0.44	0.46 ± 0.00	0.18 ± 0.00	0.25 ± 0.	405.29 ± 1.40
Je-R1	21.81 ± 0.16	0.03 ± 0.00	0.13 ± 0.00	0.17 ± 0.00	48.66 ± 0.34	0.17 ± 0.00	0.08 ± 0.00	0.09 ± 0.	151.03 ± 1.09
Kh-S2	86.29 ± 4.61	0.11 ± 0.01	0.51 ± 0.03	0.62 ± 0.04	189.5 ± 9.84	0.69 ± 0.04	0.21 ± 0.02	0.37 ± 0.02	605.37 ± 32.36
Ba-S2	58.55 ± 7.07	0.07 ± 0.01	0.34 ± 0.04	0.41 ± 0.05	124.35 ± 15.08	0.47 ± 0.06	0.14 ± 0.02	0.25 ± 0.03	416.01 ± 50.27
Kh-Pap2	91.48 ± 23.31	0.11 ± 0.03	0.49 ± 0.13	0.6 ± 0.17	180.14 ± 48.83	0.72 ± 0.18	0.22 ± 0.08	0.39 ± 0.1	666.31 ± 165.41

3.1. Environmental Pathways of Radionuclides

Insights into the possible connections between pathways of radionuclides in the environment and the human diet are one of the major purposes of this review. These figures reflect the significant difference between environmental conditions and those of food crops, highlighting the effect of geochemical and biogeochemical barriers. In here in this review, we found that Radium-226 (^{226}Ra) has shown significant availability in the environment. Although its concentration in food was much lower than that in sediments, other side its detection in papaya (Kh-Pap1,2: 43.31 Bqkg^{-1}) and leafy greens (Kh-LV1: 34.22 Bqkg^{-1}) is meaningful also. This uptake aligns with radium's chemical similarity, which is connected to calcium, allowing its absorption by plants through similar physiological mechanisms (Mitrović et al., 2016). This suggests that ^{226}Ra is the most active and available one among the natural radionuclides assessed in the local environment.

On the other hand, the concentration of ^{232}Th was negligible in the samples. Some food sample concentrations were immeasurable (Arum A1-A2) while others were low (Rice R-1: 19.4 Bqkg^{-1}). This is most likely due to the low solubility of thorium and a strong fixation on soil or sediment particles, which makes it less susceptible to absorption by plants (Fu et al., 2022). Because ^{232}Th stays in sediments for long periods of time and is less readily absorbed by plants, it appears that the primary risk of ^{232}Th exposure to mankind will occur through external irradiation and not ingestion. In the case of the vital macronutrient ^{40}K, it offers an interesting scenario here. It shows high levels in potassium-rich foods like papaya (1490.27 Bqkg^{-1}) and leafy vegetables (1110.50 Bqkg^{-1}), which reflect typical plant physiology and dietary potassium requirements, rather than its contamination. Because the remarkable high levels of ^{40}K in some sediments entail a geological event and, therefore, it holds little direct connection to the food chain in a similar way to the potassium present in agricultural soils.

Overall, the findings indicate that although the environmental reservoir in sediment hotspots is significant, the current transfer to the human diet is limited. Nevertheless, this should not foster complacency. Modifications in agricultural processes, such as the wide use of phosphate fertilizers that may contain elevated uranium series radionuclides, or changes in soil pH, could potentially enhance the mobility and plant uptake of these elements in the future, highlighting the need for continuous monitoring. These results indicate that while there is a considerable environmental hub that is held in sediment hotspots, current transfer to the human diet remains low. This does not invite complacency. Because modifications in modern agricultural practices (such as the blanket application of phosphate fertilizers that may translocate uranium series radionuclides) or changes in soil pH may effectively

enhance the mobility and plant uptake of those elements in the future, that's why it's important need for ongoing monitoring (Rashed-Nizam et al., 2014).

3.2. Radiological Health Risk Assessment: A Cause for Concern in Specific Contexts

Raw concentration data conversion shows standardized radiological hazard indices which provide a direct, accessible option for evaluating potential health hazards of dual aspects for the Khulna Division. The risk to the public of consuming local agricultural products does not appear excessive through this dietary intake. For example, arum (Kh-A1, A2), paddy (Kh-Pad1) and rice (Je-R1) always produced hazard indices under global safety standards with *AEDE* measures under 0.1 $mSvy^{-1}$, and *ELCR* estimates used in this study also generally under 1.0×10^{-4}, which is an acceptable figure (UNSCEAR, 2000). This finding provides reassurance regarding food safety in the area. Significantly different situation for the identified sediment hotspots, where the calculated indices indicate a notable radiological risk. All the sediment samples from Bagerhat (Ba-Se1) provided alarming results in terms of Ra_{eq} which is 1518.61 $Bqkg^{-1}$, H_{ext} is 4.1 and D_{out} is 794.7 $nGyh^{-1}$. The Excess Lifetime Cancer Risk was the most important index and is greater than 3.41×10^{-3} and *AGDE* greater than 5900 μSvy^{-1} which far exceeds from the recommended limits (Ekong et al., 2021; UNSCEAR, 2000). While not directly consumed, these sediments are a major and continuous source of external gamma radiation. Therefore, the most affected population are those who live in these environments for a long period, like fishermen, sediment extractors, mangrove forestry workers and farmers of these low-altitude regions. In such cases, with chronic exposure, there could be a cumulative effective dose that is considered to lead to a significant health risk. It is also possible that this contaminated sediment was re-suspended in air (as indicated by the moderate values in Kh-D1), providing an additional useful inhalation pathway that deserves further investigation. The application of age-dependent dose coefficients which were not given in the tabulated results is important to consider as the children are more radiosensitive and so could see greater relative risks from the same environmental exposure (Choudhury et al., 2022).

3.3. Spatial distribution and identification of radioactivity hotspots

The spatial distribution patterns of natural radionuclides across the Khulna Division reveal distinct regional variations, with particularly notable radioactivity hotspots detected mainly within core sediment samples from the Sundarbans and nearby delta regions. All these spatial distributions which are shown in Figure 5(a), Figure 5(b) and Figure 5(c) for radioactivity hotspots can easily indicate the concern area. Core sediments from Bagerhat (Ba-Se1, Ba-Se2) showed remarkably high activity concentrations of ^{232}Th (115.3 Bkg^{-1}), which can be identified from Figure 5(b) and an extraordinarily high level of ^{40}K (16,265.3 $Bqkg^{-1}$) Figure 5(c), both considerably above average global levels for sediments (UNSCEAR, 2000). Conversely, sediments collected from Satkhira (Sat-Se1, Sat-Se2) show relatively higher concentrations of ^{226}Ra (75.4 - 85.7 $Bqkg^{-1}$). These trends are also further verified by the spatial distribution patterns of ^{226}Ra across Khulna Division; they revealed that Bagerhat and Satkhira sediments (81–99 $Bqkg^{-1}$) had the highest activity, similar to those obtained from Table 2, where it was found that highest activity (101.3 $Bqkg^{-1}$) was observed in core sediments of Bagerhat. In the same vein, soil and other samples present activity levels of medium values (26 - 80 $Bqkg^{-1}$), whereas food like arum and leafy vegetables contain less than this value (5.77 - 34.22 $Bqkg^{-1}$). In Figure 5(a), due to the less concentration, the poor transfer of ^{226}Ra from soil to plant

is likely to be geochemically controlled, because radium is generally enriched in finer sediment fractions by hydrological and depositional mechanisms. This spatial heterogeneity suggests that environmental ^{226}Ra exposure is mainly external, with moderate plant uptake detected in specific crops due to root adsorption and soil composition. The observed spatial distribution is not random; it is fundamentally connected to the geological background of the area. The Bengal Delta, shaped by the sedimentary processes of the GBM river system, is recognized for its abundance of heavy minerals such as monazite and zircon 7.

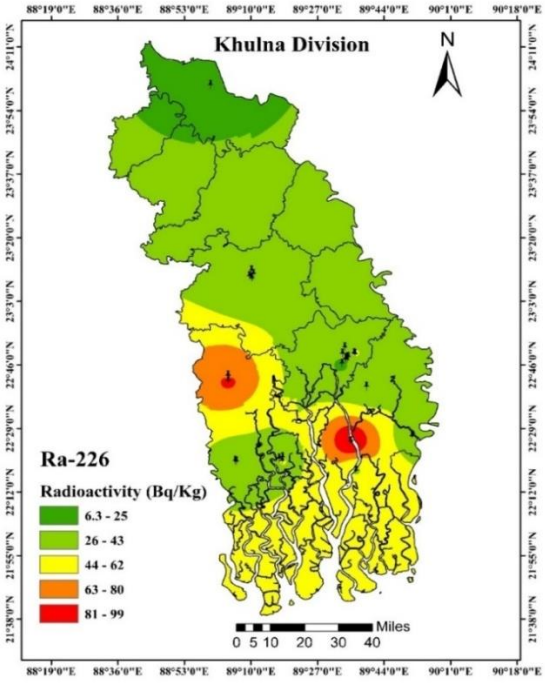

Figure 5(a). Spatial distribution map of ^{226}Ra activity concentration for different areas in Khulna Division and the red color areas indicate the maximum concentration of ^{226}Ra.

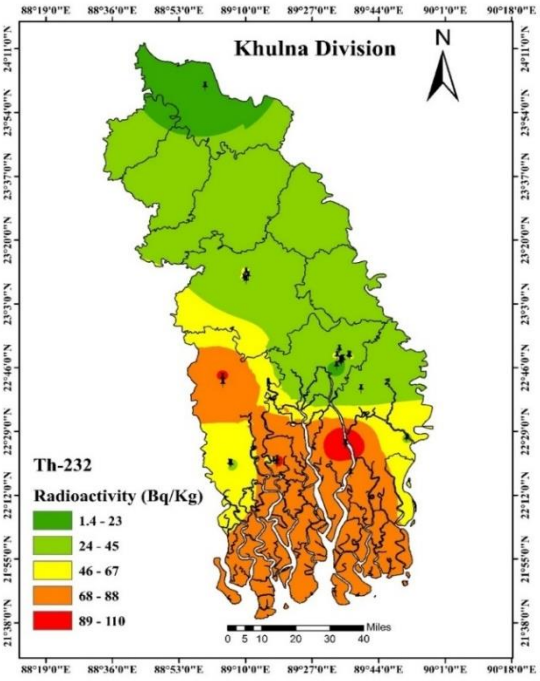

Figure 5(b). Spatial distribution map of ^{232}Th activity concentration in different areas across Khulna division.

These minerals are the main hosts of thorium and uranium decay series, explaining in part why ^{232}Th and ^{226}Ra were elevated in these deltaic deposits. Thorium has a similar distribution pattern to uranium, but it is chemically more constrained and its maximum concentrations occur in the southern deltaic areas with Bagerhat and Satkhira showing the highest levels ranging from 89 Bqkg^{-1} to 110 Bqkg^{-1}.

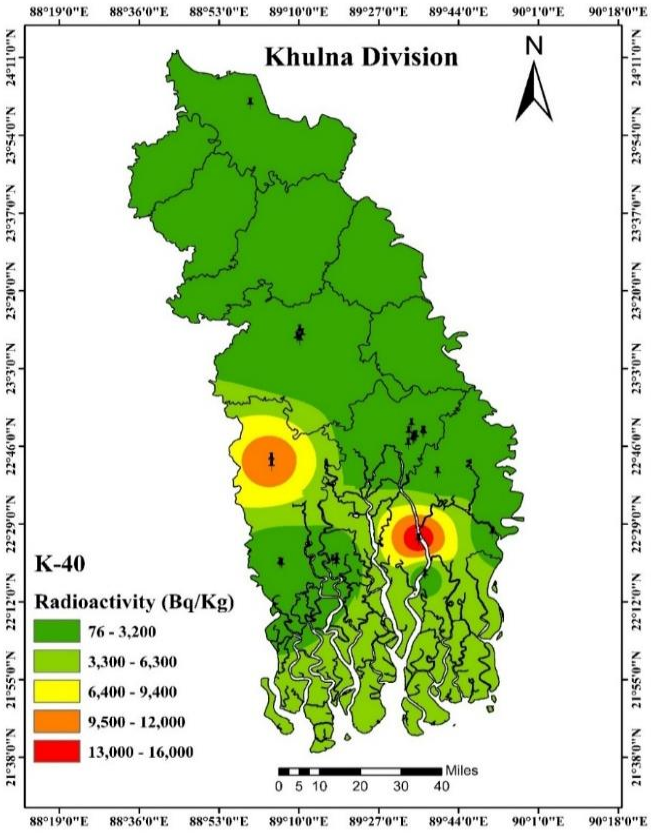

Figure 5(c). Spatial distribution map of ^{40}K activity concentration in different regions of Khulna Division, showing the maximum and minimum radioactivity of ^{40}K.

These hotspots correspond to the high values found in Table 2 of up to 115.3 Bqkg^{-1} for Bagerhat core sediments. The activity on the ground is usually a moderate one (33 - 77 Bqkg^{-1}), with food samples containing low thorium contents frequently less than 20 Bqkg^{-1}. Weak soil-to-plant transfer and minimal bioavailability of ^{232}Th are caused by its strong sediment binding and low solubility. Consequently, the dominant exposure pathway for thorium is external radiation rather than ingestion. The results elevated the radioactivity in that deltaic sediments correlates with these higher radiological hazard indices (Ra_{eq} and absorbed gamma dose rates), which exceed international safety limits and underscore external exposure risks among communities dependent on these environments. The high concentration of ^{40}K likely reflects the deposition of potassium-rich minerals like feldspar and mica in certain sedimentary settings. Additionally, research indicates that catastrophic occurrences, such as Cyclone Aila, can substantially modify sediment profiles by redistributing and concentrating these radionuclide-bearing minerals (Arafin et al., 2020; Tasnim Nijhum et al., 2021). This points out that the enriched hotspots derive from complex natural geochemical enrichment processes. Meanwhile, ^{40}K has a more extensive natural and biological occurrence. Average soil and sediment activity levels are reasonably moderate (225-881 Bqkg^{-1}), although certain core sediments from Bagerhat and Satkhira show extremely high values which exceeding 13,000 Bqkg^{-1} compared to

Table 2's recorded hotspot value of 16,265.3 $Bqkg^{-1}$. Food crops included papaya and leaves also show a higher ^{40}K activity (up to 1490.27 $Bqkg^{-1}$) than paddy does and indicating potassium as metabolic element for plants rather than radionuclides contamination. The radiological dose calculation reveals that the food-borne exposure is still much lower than those at safety limits (AEDE < 0.1 mSv/year; ELCR < 1×10^{-4}).

Nevertheless, in the common point of local ^{226}Ra and ^{232}Th hotspots, the environmental ^{40}K content highlights Bagerhat-Satkhira delta as an area that needs to remain under continuous radiological monitoring. In contrast, inland agricultural and rural soil samples such as Kushtia (Ku-S1) and a few locations in Jessore (Je-S2) showed radionuclide concentrations in good agreement with the worldwide background levels. Urban samples such as road dust from Khulna City (Kh-D1), showed moderate enrichment that can be attributed to natural soil re-suspension and minor anthropogenic inputs from industrial and urban activities.

This distinct spatial difference between these high-risk sedimentary areas and lower-risk inland regions are essential for guiding environmental monitoring efforts and developing targeted and cost-efficient public health strategies. Thus, spatial mapping site-specific the ^{226}Ra, ^{232}Th, and ^{40}K as crucial for effective environmental risk management and safeguarding public health against chronic external radiation exposure.

3.4. Comparative Assessment of AACED and ELCR across Age Groups

The Figure 6(a) and Figure 6(b) together show comparative trends of the AACED and the ELCR across all the food samples analyzed as different as three demographic groups: adults, children and infants shown in Table 3. As visualization in Figure 6(a), adults consistently have higher AACED values compared to children and infants, which highlights the age-related differences in radiation dose intake and biological vulnerability. Adults present the highest average AACED values that attributed to increased environmental exposure and lifestyle or occupational activities by higher rates of inhalation or ingestion as indicated in previous research on natural radionuclide exposure patterns (ICRP, 2007; UNSCEAR, 2022). Children with their smaller body mass and shorter exposure durations demonstrate intermediate dose levels whereas the infants display the lowest AACED. It reflects their limited interaction with the environment and reduced cumulative exposure times. These findings support established radiological concepts that suggest effective dose is related to both exposure rates and biological intake factors (IAEA, 2014, 2018).

In Figure 6(b), the ELCR values obtained from AACED reflect a similar decreasing pattern across the various age groups. Nevertheless, the ELCR values for infants are essentially zero at all sampling locations, a condition resulting from the minimal cumulative dose noted during the early stages of life. This nearly null risk does not suggest an absolute absence of effects but rather indicates that, according to the linear no-threshold (LNT) model used in radiological risk evaluations, the level of exposure is too low to yield a significant statistical increase in the likelihood of developing cancer over a lifetime (Jafarian-Dehkordi & Hoeschen, 2025; Jargin, 2024). ELCR values for the adult were notably higher due to longer exposure times, increased metabolic uptake and cumulative effects over lifelong exposure. From a public health standpoint, this implies that attention in radiological protection and environmental remediation to adult as well as child populations will be important for long-term health risk.

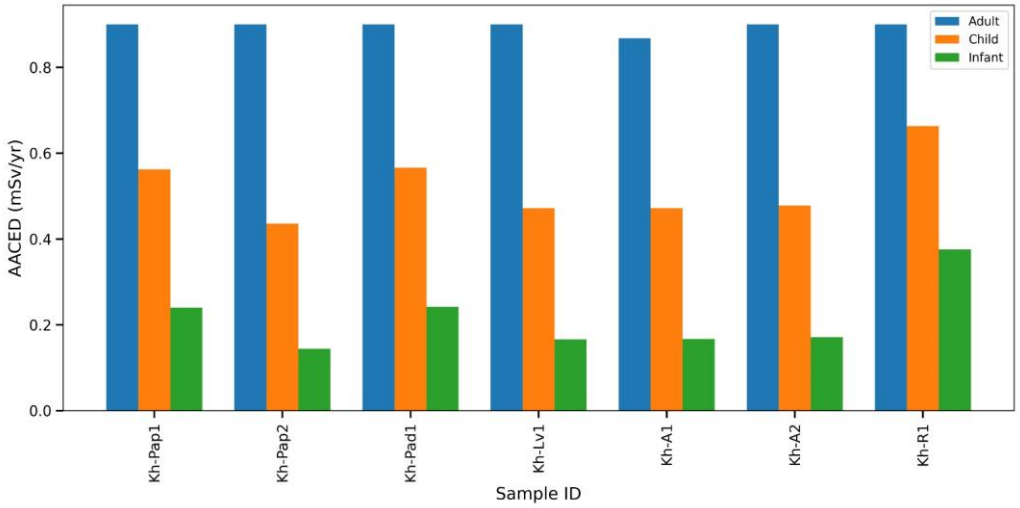

Figure 6(a). Comparison between Annual Average Committed Effective Dose (AACED) for (adult, children and infant), expressing the exposure rate to radioactivity.

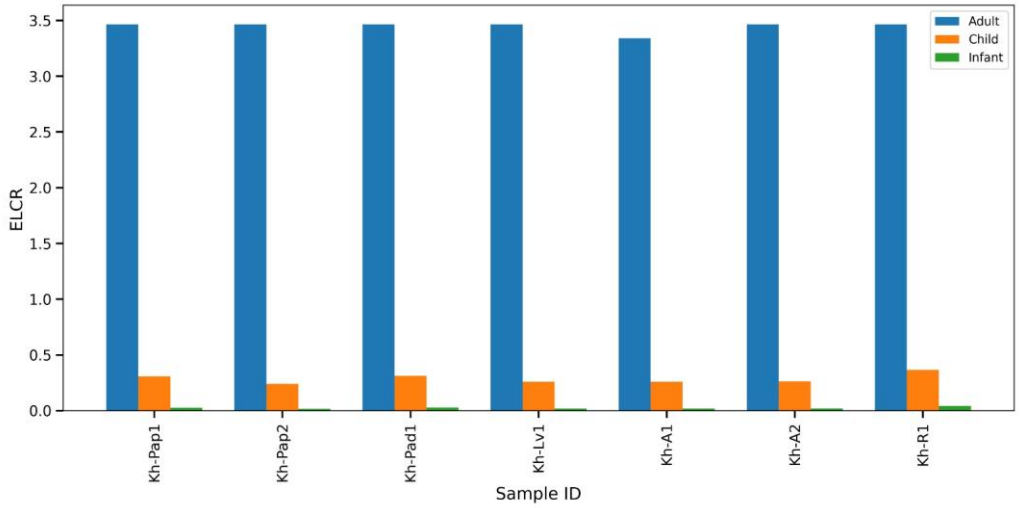

Figure 6(b). Comparison between Excess Lifetime Cancer Risk (ELCR) for adult, children and infant, which represent the cancer risk for different ages.

On the other hand, the low value of ELCR for newborns underscores the importance of accurate lifetime dose estimates and demonstrates how policies towards early-lifetime protection are successful in reducing stochastic radiation risks below levels considered acceptable (ICRP, 2007; UNSCEAR, 2000).

4. Conclusion

This comprehensive review has crumbled data to give an ample overview of the environmental radioactivity level in Khulna Division of Bangladesh. This spatial analysis and appraisements of radiological risk, measured by gathering data from soil, sediment, dust, and essential food crops, has effectively filled significant research gaps and achieved its main objectives. The findings of this study point out the area in different radiological terrain. Strong natural radioactivity hotspots have been highlighted, especially in the deltaic sediments of Bagerhat and Satkhira, due to the geogenic aggregation of heavy minerals. These epicenters show the radiological hazard indices, specifically ELCR and AGDE, which exceed international safety standards and emphasize potential health risk for

people who are exposed to these sediments for an extended period of time. Furthermore, the section of ecosystem pathways shades a more optimistic picture regarding the food chain. Nowadays, the shifting of radionuclides from ^{232}Th in soil to locally produced food crops is minimal. Therefore, the radiological risks due to the intake of these staple foods (rice, arum and leafy greens) are considered safe for the general population. The study sets crucial baselines for observing the environmental radioactivity in Khulna Division. It mainly focuses on a dualistic approach: first, the implementation of specific surveillance and mitigation strategies in the highlighted sediment hotspots to protect the occupationally disclosed groups; and secondly, monitoring the food chain and environmental elements to easily identify any changes in radionuclides transfer because of human activities or climate change. The techniques used here, particularly the merging of gamma spectrometry with GIS offer a vigorous model to determine the evaluation of our environment, both ecologically sensitive and rapidly evolving areas. Eventually, the accumulated information in this review is crucial to being known by policymakers, environmental organizations and public health authorities for creating evidence-based approaches for sturdy development, radiation safety and safeguarding human and ecosystem health in Khulna Division.

5. Recommendations for Future Research

1) Monitoring of radionuclides in major areas and control areas of the Khulna Division over a long-term basis.

2) Sample collection from sediment core samples which will include Uranium/Thorium and other artificial radionuclide series.

3) Identification of hotspots using Geostatistical GIS Mapping, Uncertainty Testing and Kriging.

4) Utilizing combined data of Radionuclide and Mineralogical and Geochemical characteristics to trace back the source of the Radionuclide in the soil.

5) Radioecological information on Transmission of Soil to Crop and on the local Crop Basket under Agricultural and Dietary Conditions.

6) Assessment of Epidemiological and biomarker in higher exposure areas to define age dependent health risks.

Declarations

Source of Funding

This study received no specific grant from any funding agency in the public, commercial, or not-for-profit sectors.

Competing Interests Statement

The authors declare that they have no competing interests related to this work.

Consent for publication

The authors declare that they consented to the publication of this study.

Authors' contributions

All the authors took part in literature review, analysis, and manuscript writing equally.

Availability of data and materials

Supplementary information is available from the authors upon reasonable request.

Institutional Review Board Statement

Not applicable for this study.

Informed Consent

Not applicable for this study.

Acknowledgements

We the authors would like to express our heartfelt gratitude to Research Buddy AI platform for providing a great opportunity to carry out this work. We are also grateful to Md. Abadat Hossain for his great supervision, insightful guidance, and continuous encouragement throughout this study. His expertise and patience in this field were crucial in bringing this manuscript to successful completion.

References

[1] Absar, N., Rahman, M.M., Kamal, M., Siddique, N., & Chowdhury, M.I. (2014). Natural and anthropogenic radioactivity levels and the associated radiation hazard in the soil of Oodalia Tea Estate in the hilly region of Fatickchari in Chittagong, Bangladesh. Journal of Radiation Research, 55: 1075. https://doi.org/10.1093/jrr/rru054.

[2] Arafin, S.A.K., El-Taher, A., Fazlul Hoque, A.K.M., Ashraful Hoque, M., Ferdous, J., & Joynal Abedin, M. (2020). Natural gamma radiation level detection in agriculture soil after Aila disaster and comparison with deep soil gamma activity in a specific area of Sundarban region, Satkhira, Bangladesh. International Journal of Radiation Research, 18: 397–404. https://doi.org/10.18869/acadpub.ijrr.18.3.397.

[3] Arafin, S., Akramuzzaman, M., & Hoque, A. (2016). Terrestrial gamma ray activity in soil from Aila affected two upazila at Khulna and Bagerhat district. International Journal of Advanced Research and Review, Pages 10–18.

[4] Chinnaesakki, S., Bara, S.V., Sartandel, S.J., Tripathi, R.M., & Puranik, V.D. (2012). Performance of HPGe gamma spectrometry system for the measurement of low-level radioactivity. Journal of Radioanalytical and Nuclear Chemistry, 294: 143–147. https://doi.org/10.1007/s10967-011-1607-8.

[5] Choudhury, T.R., Ferdous, J., Haque, M.M., Rahman, M.M., Quraishi, S.B., & Rahman, M.S. (2022). Assessment of heavy metals and radionuclides in groundwater and associated human health risk appraisal in the vicinity of Rooppur nuclear power plant, Bangladesh. Journal of Contaminant Hydrology, 251: 104072. https://doi.org/10.1016/j.jconhyd.2022.104072.

[6] Dickson-Agudey, P., Tettey-Larbi, L., Adjei-Kyereme, S., Lawluvi, H., Asare, E.O., Osei, R.K., Ampene, A.A., & Shahrokhi, A. (2026). Radiological risk assessment of natural radioactivity in imported rice consumed in Ghana and its implications for food safety and public health. Scientific Reports. https://doi.org/10.1038/s41598-026-37317-0.

[7] Ehsan, M.S., Rahman, M.F., Tabassum, N., Prodhan, M.M.H., Pervin, S., Siraz, M.M., Rahman, A.M., Yeasmin, S., & Mahal, S.F. (2019). The activity concentration of radionuclides (226Ra, 232Th and 40K) in soil samples and associated health hazards in Natore, Kushtia and Pabna district of Bangladesh. Journal of Bangladesh Academy of Sciences, 43: 169–180. https://doi.org/10.3329/jbas.v43i2.45738.

[8] Eke, B.C., Akomolafe, I.R., Ukewuihe, U.M., & Onyenegecha, C.P. (2024). Assessment of radiation hazard indices due to natural radionuclides in soil samples from Imo State University, Owerri, Nigeria. Environmental Health Insights, 18: 1–9. https://doi.org/10.1177/11786302231224581.

[9] Ekong, G.B., Akpa, T.C., Umaru, I., Akpaowo, M.A., Yusuf, S.D., & Benson, N.U. (2021). Baseline radioactivity and associated radiological hazards in soils around a proposed nuclear power plant facility, South-South Nigeria. Journal of African Earth Sciences, 182: 104289. https://doi.org/10.1016/j.jafrearsci.2021.104289.

[10] Fu, Q., Lai, J.L., Li, C., Ji, X.H., & Luo, X.G. (2022). Phytotoxicity mechanism of the natural radionuclide thorium in *Vicia faba*. Journal of Hazardous Materials, 424: 127718. https://doi.org/10.1016/j.jhazmat.2021.127718.

[11] Henrico, I., Henrico, S., le Roux, R., & Bezuidenhout, J. (2023). Radiometric mapping of the Berg River estuary. Transactions in GIS, 27: 105–114. https://doi.org/10.1111/tgis.13011.

[12] Hossain, S., Pervin, S., Lubna, L., Karmaker, S., Yeasmin, S., & Khandaker, M.U. (2024). Transfer factors of naturally occurring radionuclides from soil-to-rice cultivated in Bangladesh and associated health implications. Heliyon, 10: e38004. https://doi.org/10.1016/j.heliyon.2024.e38004.

[13] IAEA (2014). Radiation protection and safety of radiation sources: International basic safety standards. https://doi.org/10.61092/iaea.u2pu-60vm.

[14] IAEA (2018). Radiation protection of the public and the environment.

[15] ICRP (2007). The 2007 recommendations of the International commission on radiological protection. Elsevier.

[16] Islam, N. (2016). Study on probable radionuclide contents and their dose assessment in sand, soil and water samples collected from the Rupsha River, Khulna. http://dspace.kuet.ac.bd/handle/20.500.12228/153.

[17] Jafarian-Dehkordi, F., & Hoeschen, C. (2025). Low-dose radiation risk in medicine: A look at risk models, challenges, and future prospects. Zeitschrift für Medizinische Physik. https://doi.org/10.1016/j.zemedi.2025.07.002.

[18] Jargin, S.V. (2024). Overestimation of medical consequences of low-dose radiation exposures and over-treatment of cancer. Journal of Health Science Research, 9. https://doi.org/10.25259/jhsr_36_2023.

[19] Sultana Jolly, N., Nahar, N., Paul, D., & Ali, I. (2018). Measurement of 226Ra, 232Th and 40K in arum grown on the bank of Rupsha River, Khulna, Bangladesh using HPGe detector. Jahangirnagar University Journal of Science, 41: 57–66.

[20] Kabir, K.A., Islam, S.M.A., & Rahman, M.M. (2009). Distribution of radionuclides in surface soil and bottom sediment in the district of Jessore, Bangladesh and evaluation of radiation hazard. Journal of Bangladesh Academy of Sciences, 33: 117–130. https://doi.org/10.3329/jbas.v33i1.2956.

[21] Kabir, S., Islam, M.A., & Hossen, M.B. (2024). Natural radioactivity in soils and medicinal plants of the Sundarban: Concomitant radiological risks and radionuclide transfer factor. Journal of Radiation Research and Applied Sciences, 17: 101071. https://doi.org/10.1016/j.jrras.2024.101071.

[22] Kashparov, V., Levchuk, S., Zhurba, M., Protsak, V., Khomutinin, Y., Beresford, N.A., & Chaplow, J.S. (2018). Spatial datasets of radionuclide contamination in the Ukrainian Chernobyl exclusion zone. Earth System Science Data, 10: 339–353. https://doi.org/10.5194/essd-10-339-2018.

[23] Khan, R., Akhi, S.Z., Khan, M.H.R., Sultana, S., Aldawood, S., Basir, M.S., Parvez, M.S., Naher, K., Habib, M.A., Idris, A.M., & Roy, D.K. (2025). Comparison of environmental radioactivity in road dust between a city and a megacity: Geo-environmental evaluation, health risks, and potential remediation. Environmental Toxicology and Chemistry, 44: 344–362. https://doi.org/10.1093/etojnl/vgae027.

[24] Lee, S.Y., Lim, S.H., & Kim, H.S. (2024). Assessing the radon exposure variability and lifetime health effects across indoor microenvironments and sub-populations. Atmosphere, 15. https://doi.org/10.3390/atmos15080927.

[25] Mitrović, B., Ajtić, J., Lazić, M., Andrić, V., Krstić, N., Vranješ, B., & Vićentijević, M. (2016). Natural and anthropogenic radioactivity in the environment of Kopaonik mountain, Serbia. Environmental Pollution, 215: 273–279. https://doi.org/10.1016/j.envpol.2016.05.031.

[26] Mphaga, K.V., & Rathebe, P.C. (2026). Environmental radioactivity associated with mining in Africa: Sources, levels, and health risks—A systematic review. International Journal of Environmental Health Research, Pages 1–22. https://doi.org/10.1080/09603123.2026.2621063.

[27] Nahar, N. (2016). Study of radioactivity levels in different kinds of food stuff grown on the bank of Rupsha River and its impact on human health. http://dspace.kuet.ac.bd/handle/20.500.12228/176.

[28] Wallbrink, P.J., & Murray, A.S. (2002). Radionuclide measurement using HPGe gamma spectrometry. https://doi.org/10.1007/0-306-48054-9_5.

[29] Rashed-Nizam, Q.M., Rahman, M.M., Kamal, M., & Chowdhury, M.I. (2014). Assessment of radionuclides in the soil of residential areas of the Chittagong metropolitan city, Bangladesh and evaluation of associated radiological risk. Journal of Radiation Research, 56: 22–29. https://doi.org/10.1093/jrr/rru073.

[30] Shahbazi-Gahrouei, D., Gholami, M., & Setayandeh, S. (2013). A review on natural background radiation. Advanced Biomedical Research, 2: 65. https://doi.org/10.4103/2277-9175.115821.

[31] Siraz, M.M.M., Al Mahmud, J., Alam, M.S., Rashid, M.B., Hossain, Z., Khandaker, M.U., Bradley, D.A., Miah, M.M.H., Alshahrani, B., & Yeasmin, S. (2023). Risk assessment of naturally occurring radioactivity in soil adjacent to a coal-fired brick kiln. Radiation Physics and Chemistry, 209: 110985. https://doi.org/10.1016/j.radphyschem.2023.110985.

[32] Siraz, M.M.M., Islam, S., Shelley, A., Alam, M.S., Mahmud, A., Rashid, M.B., Khandaker, M.U., Yeasmin, S., & Rahman, M.S. (2025). Radioactivity distribution and concomitant hazards evaluation of industrial zones soils from Chattogram, Bangladesh: A multivariate statistical analysis. PLOS ONE, 20: e0328356. https://doi.org/10.1371/journal.pone.0328356.

[33] Siraz, M.M.M., Jubair, A.M., Alam, M.S., Rashid, M.B., Hossain, Z., Khandaker, M.U., Bradley, D.A., & Yeasmin, S. (2023). Measurement of radioactivity in soils of Karamjal and Harbaria mangrove forest of Sundarbans for establishment of radiological database. PLOS ONE, 18: e0289113. https://doi.org/10.1371/journal.pone.0289113.

[34] Tasnim Nijhum, Z., Amirul Islam, M., & Nahid, F. (2021). Assessment of natural radioactivity and radiological health hazards in core sediments of the Sundarbans using gamma-ray spectrometry. IOSR Journal of Applied Physics, 13: 19–29. https://doi.org/10.9790/4861-1305031929.

[35] UNSCEAR (2000). Sources and effects of ionizing radiation. United Nations Scientific Committee on the Effects of Atomic Radiation.

[36] UNSCEAR (2022). Sources, effects and risks of ionizing radiation. United Nations Publication.

[37] Uzochukwu Leonard, A., & Ikenna Emmanuel, O. (2022). Estimation of utilization index and excess lifetime cancer risk in soil samples using gamma ray spectrometry in Ibolo-Oraifite, Anambra State, Nigeria. American Journal of Environmental Science and Engineering, 6: 71. https://doi.org/10.11648/j.ajese.20220601.21.

[38] Wong, E., Tan, H.J., Corcho-Alvarado, J.A., Loh, E., Ong, J., Ong, C.Y., Toh, D., Röllin, S., Gosteli, R., Sahli, H., Furrer, V., Kradolfer, S., Ossola, J., Von Gunten, C., & Stauffer, M. (2025). Natural and anthropogenic radionuclides in selected environmental radioactivity monitoring sites in Singapore. Journal of Radioanalytical and Nuclear Chemistry, 334: 1433–1443. https://doi.org/10.1007/s10967-024-09920-w.

[39] Yang, Q., Ding, C., Zhao, X., Hu, S., Shao, Y., Zhai, J., & Zhang, Q. (2025). Environmental radiological monitoring and risk assessment in shale gas areas. Environmental Research, 286: 122768. https://doi.org/10.1016/j.envres.2025.122768.